Fabrication of Poly(lactic acid) Microspheres with Various Micro-Structure by Microfluidic T-junction and Gelatin Pore-forming Agent

Yanjun Bai,[a] Feng Liu,[b] Yifan Zhang,[b] Lei Wu,[b] Haihu Liu,[b] and Yan Ba [a,*]

Microporous-structured Poly(L-lactic acid) (PLLA) spheres were fabricated using a microfluidic shearing method. Poly(vinyl alcohol) (PVOH) solution is used as the continuous phase, and an emulsion containing matrix materials (PLLA), stabilizer (polysorbate 80) and pore-forming agents (gelatin) dissolved in dichloromethane (DCM) were emulsified to be dispersed phase for the generation of droplets, which were eventually transformed into microspheres. An ice water bath environment was shown to be necessary to produce stable microspheres. In addition, it was found that the mechanical stirring emulsification method was more conducive to microstructure construction than the ultrasonic emulsification. By regulating the amount of pore-forming agent (2.5 wt%, 5 wt%, and 7.5 wt% gelatin), three types of micro pores (small: 2.9±0.8 μm, middle: 46.9±14.9 μm, and large: 127.3±55.3 μm) on surface with different inner structure were obtained. Finally, it was demonstrated that the proposed method is general enough to prepare various other polymer microspheres such as PNAGA (Poly-N-acryloyl glycinamide) and PCL (Polycaprolactone).

DOI: 10.15376/biores.20.4.9063-9078

Keywords: Microfluidic; Emulsification; Micro-pore structure; Polymer spheres

*Contact information: a; National Key Laboratory of Solid Rocket Propulsion, School of Astronautics, Northwestern Polytechnical University, 127 West Youyi Road, Xi'an 710072, China; b: School of Energy and Power Engineering, Xi'an Jiaotong University, 28 West Xianning Road, Xi'an 710049, China; *Corresponding author: bayan@nwpu.edu.cn*

INTRODUCTION

The regulation of microstructure plays a vital role in the realization of material functions. Microstructures such as porous structure (Elsayed *et al*. 2016; Zeng *et al*. 2021), hollow structure (Deng *et al*. 2017), and fibrous structure (Wu *et al*. 2013) can effectively increase the specific surface area of materials, thereby enabling the effective transport and delivery of substances inside the material structures (Purbia and Paria 2015; Sommer *et al.* 2016; Solsona *et al.* 2019). The main method to fabricate microstructure spheres is the thermally induced phase separation method (Barroca *et al*. 2010; Nie *et al*. 2017). The materials with microstructure facilitate the enormous applications in the fields of biomedicine, energy conversion and storage, anti-pollution and purification, and porous structure insulation materials to reduce the negative mass in a solid rocket motor. Therefore, the regulation of micro/nano structures has attracted the continuous attention of researchers in the past years.

Since the advent of microfluidic technology, it has been shown to have significant advantages such as high sensitivity and high accuracy when induced into chemical synthesis or physical preparation (Ježková *et al*. 2022; Liu *et al*. 2022; Maeki *et al*. 2022;

Zou *et al*. 2022). The operational accuracy at the microscale or nanoscale level enables the preparation based on microfluidic technology to greatly improve the regulation effect and the probability of generating target product. Therefore, it is particularly important to regulate the preparation process of various structural materials based on microfluidic technology, such as the preparation of complex micro- or nano-structured microparticles. The existing studies on the use of microfluidic technology for manufacturing microscale or nanoscale particles mainly have focused on the regulation of overall size and shape, such as microspheres with 100 nm (Li *et al*. 2021; Zou *et al*. 2022; Jing *et al*. 2023) or microspheres with the size ranging from 10 to 100 μm (Aghaei *et al.* 2021; Zhao *et al.* 2021b), spherical particles (de Carvalho *et al*. 2021; Zhao *et al*. 2021a), rodlike particles (Visaveliya and Kohler 2014), Janus particles (Bao *et al*. 2020; Dai *et al*. 2021), and star shaped particles (Fales *et al*. 2011). Benefiting from the rapid transfer of mass and energy, the products manufactured using microfluidic technology often perform better than those prepared from traditional methods. At the same time, microfluidic technology is increasingly used to fabricate complex structured particles, such as porous spheres, hollow spheres, and stacked structured particles.

However, the microfluidic preparation used for complex structured particles suffers from several challenges. The greatest challenge is the selection of structural regulators. Different matrix and structure require different structure regulation agents, and the choosing of structure regulation agent in microfluidic technology is much more difficult (Wang *et al*. 2015; Xu *et al*. 2009). The second challenge is to protect the integrity of the prepared particles, as the more complex the structure of micro- and nano-particles are, the lower are their structural stability, and thus the higher requirements are needed for ensuring the structural stability and non-fragmentation (Geng *et al*. 2020; Tahira *et al*. 2020; Joseph *et al*. 2022). In addition, how to ensure the universality of the preparation method and its prospects in commercial production is also a challenging task and deserves widespread attention (Geng *et al*. 2020; Zhao *et al*. 2020; Shoji *et al*. 2021).

To tackle the above challenges, this study explored the preparation of poly-L-lactic acid (PLLA) porous microspheres as an example of what can be accomplished using a comprehensive microfluidic preparation process. PLLA is a polyester synthesized *via* ring-opening polymerization of lactide, and PLLA porous microspheres, with their great mechanical properties, high porosity and large surface area, have attracted the attention of researches in biological applications (Zeng *et al*. 2021). To prepare such PLLA spheres with porous microstructure, several steps should be addressed, including the microfluidic preparation of PLLA droplets (Kim *et al*. 2018; Prasad *et al*. 2009; Ziemecka *et al*. 2011), solidification process (Shi and Weitz 2017; Werner *et al*. 2021), and the generation of porous microstructure (Nie *et al*. 2017). In the present work, a preparation method was set up that can successfully produce PLLA spheres with different sizes of porous microspheres. In the method, PLLA, the stabilizer, together with the pore-forming agent (gelatin) are dissolved in dichloromethane (DCM) by the emulsion method of mechanical stirring to form a dispersed phase, which is then sheared to droplets by use of a T-junction microfluidic shearing device. Droplets were solidified *via* DCM volatilization in an ice-water bath (0 °C), followed by the removal of pore-forming agent in a hot-water bath (50 °C) to form porous microspheres. Through the experiments, various process parameters, including emulsification process, droplet collection environment, pore-forming agent dosage, stabilizer (*i.e.*, surfactants), and universality of preparation process were evaluated. A reliable microfluidic preparation process for PLLA spheres with small (2.9±0.8 μm), middle (46.9±14.9 μm), and large (127.3±55.3 μm) pore structures was identified. Such a

microfluidic process is also suitable for preparing porous microspheres with similar polymer matrices, such as poly-N-acryloyl glycinamide (PNAGA) and polycaprolactone (PCL). In future work, the authors plan to further explore the universality of the present method and adapt the method to other polymers such as polyglycolide (PGA), poly lactic-co-glycolic acid (PLGA), and poly(N-isopropylacrylamide) (PNIPAM), as well as biopolymers such as cellulose derivatives. Hopefully, the proposed design strategy could be extended to the preparation of more complex structural materials for high-tech applications.

EXPERIMENTAL

Materials

The macromolecules used in the microfluidic synthesis included PLLA (molecular weight $M_n \cong 220$ kiloDalton, PCL ($M_n \cong 80$ kiloDalton), and PVOH (polyvinyl alcohol, $M_n \cong 31$ kiloDalton, 87% hydrolyzed) and PNAGA ($M_n \approx 31\ k$), which were purchased from Shanghai Macklin Biochemical Co., Ltd. Other reagents such as Span 80 (polysorbate 80), gelatin, and ethanol were acquired from China National Medicines Co., Ltd., and DCM (dichloromethane) and dimethylsilicone oil were purchased from Chengdu Chron Chemical Co. Ltd. These chemicals were all used as received without any further purification. MilliQ water was prepared using a MilliQ system (Bedford, MA, America).

Microfluidic Devices

As shown in Scheme 1, the microfluidic reactor consisted of two parts: a microreactor and a post-treating module. The micro-reactor is made of a T-shaped channel and high precision micro-pumps. All the channels were of equal width W and depth h, *i.e.*, $W = h = 600$ μm, with the size error within 1% and the channel roughness less than 1.0 μm. The PTFE tube with an inner diameter of 600 μm and an outer diameter of 800 μm was used to connect post-treating module. The T-shaped channel contains two inlets used to feed emulsion and PVOH solution, which are the dispersed phase and the continuous phase, respectively.

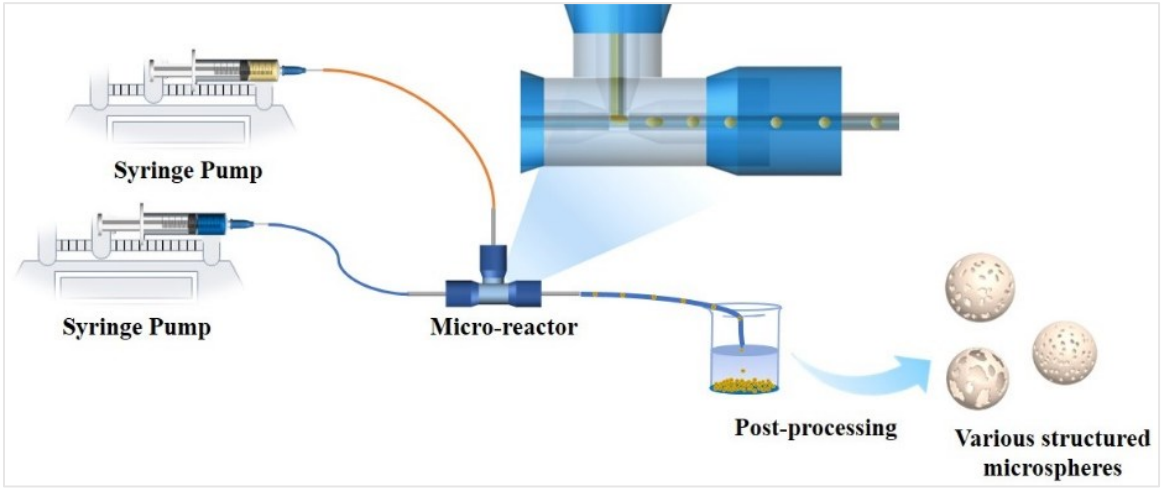

Scheme 1. Illustration of the fabrication process used for various structural microspheres

The dispersed phase is composed of matrix materials, appropriate dosage of pore forming agent and surfactants. The droplets were generated from the dispersed phase under the shear action of the continuous phase and ultimately transformed into micro-spheres in the post-treating module. The PTFE tube with inner diameter of 600 μm and outer diameter of 800 μm was used to connect the micro-reactor with the post-treating module. The post-treatments include applying a specific surrounding temperature to collect droplets and maintain morphological stability, several hours stewing for DCM volatilization, and hot water bath with stirring for achieving specific dissolution of the pore-forming agent and thus for pore formation. The final product was obtained by washing multiple times with deionized water followed by freeze drying. In the post-treating module, three different surrounding temperatures were considered. The temperatures were achieved by leading the droplets into a beaker containing liquid nitrogen, ice water, or room temperature water, respectively.

Preparation of PLLA Spheres

As stated above, the droplets are generated in the T-shaped channel and collected in the beaker for a certain surrounding temperature, and then the emulsion droplets are solidified through the volatilization of DCM in the droplets to obtain the spheres. Considering that DCM is the oil phase, and the pore-forming agent is required to be insoluble in DCM but completely dissolved in hot water to achieve the purpose of pore formation, gelatin was selected as the pore-forming agent in the experiment. According to the previous works (Prasad *et al.* 2009; Ziemecka *et al.* 2011; Liu *et al.* 2016; Kim *et al.* 2018; Zhou *et al.* 2021), the flow rate ratio of continuous phase to dispersed phase was set to 5:1, corresponding to the flow rates 250 μL/min for continuous phase and 50 μL/min for dispersed phase. About 1.0 g DCM containing 5 wt% PLLA and 7.5 wt% Span 80 and 5 g of 1 wt% poly(vinyl alcohol) (PVOH) solution (without gelatin) were mixed in a small beaker, and ultrasonic emulsification was used for 30 min to obtain emulsion as dispersed phase, which was then loaded into a 10 mL syringe. In addition, 50 mL 1.0 wt% PVOH solution, as continuous phase, was loaded into a 50 mL syringe. During the collection and solidification process of droplets, the surrounding temperature has a significant impact on the product morphology. Therefore, three different surrounding temperatures were tested, namely ultra-low temperature (liquid nitrogen bath), low temperature (ice water bath), and room temperature (room temperature water bath).

Fabrication of Microspheres with Specific Micro-structure

Initially 0.05 g PLLA and 0.075 g sorbitan monooleate (Span 80) were dissolved in 1.0 g of DCM. Meanwhile, different dosages (0 wt%, 2.5 wt%, 5wt%, 7.5 wt%, 10 wt%) of the pore-forming agent gelatin, was dissolved in 5 g deionized water. The resulting two solutions were then mixed and emulsified by different methods (ultrasonic emulsification with the frequency of 20 kHz for 30, 10, 5, and 1.0 min and high-speed at 2500 rpm mechanical stirring for 30 and 5 min), leading to the dispersed phase. The continuous phase used was 1.0 wt% PVOH solution. Droplets generated by the micro-reactor were collected and imported into a beaker for liquid nitrogen bath, ice water bath, or room temperature water bath. After four hours of stewing, the organic reagent DCM totally volatilized, and the droplets were transformed into solid spheres in the solution. The hot water bath (50 °C) with continuous stirring was followed to remove pore-forming agent and thus form porous structure. Then, the spheres were washed three times with deionized water, and finally

dried through freeze-drying. In addition, to show its universality, the present method was also extended to the preparation of PCL and PNAGA microspheres.

Characterization

Scanning electron microscopic (SEM) images were taken using a JEOL 7800F scanning electron microscope operated at 3 kV. Fourier transform infrared (FTIR) spectra were collected on a Nicolet iS50 FTIR spectrometer. The pore size and size distribution were detected and calculated by the open-source software Image J.

RESULTS AND DISCUSSION

Effects of the Selected Surrounding Temperature

Figure 1 shows photographs of the droplets and the SEM images of the final PLLA microspheres under three different surrounding temperatures. In the ultra-low temperature environment, corresponding to liquid nitrogen bath, the droplets and their surrounding continuous phase were rapidly frozen, presenting ice pellets larger than the droplets. The freezing of the continuous phase was extremely destructive to the morphology of the final PLLA spheres, which can be observed in Fig. 1 (d).

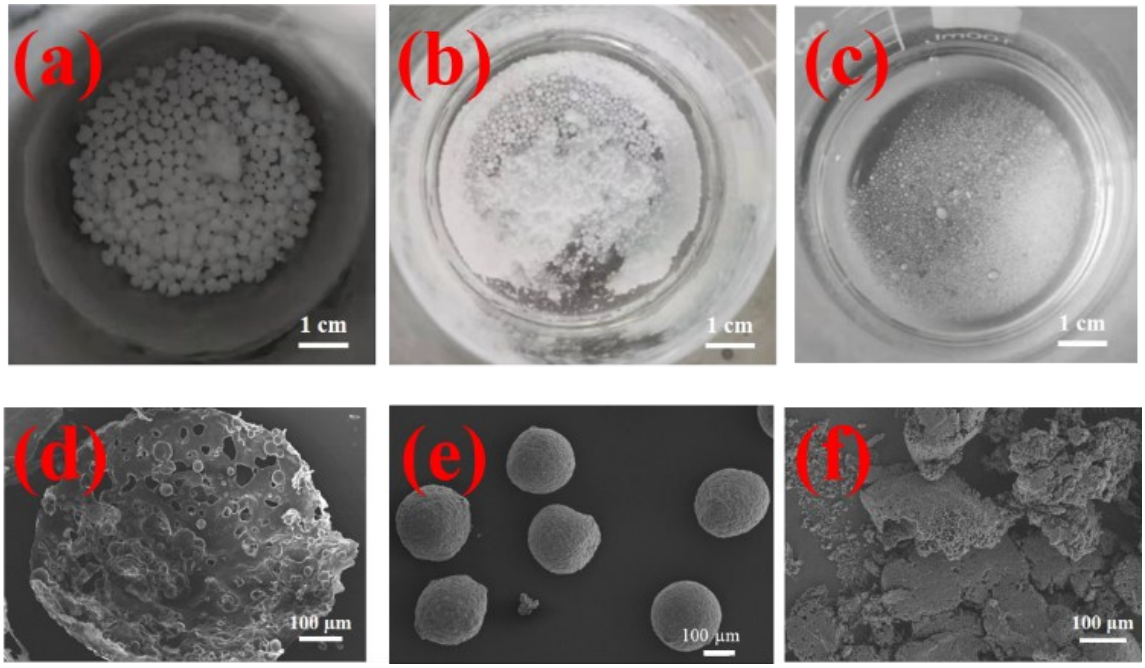

Fig. 1. Photographs of droplets obtained by (a) liquid nitrogen bath, (b) ice water bath, and (c) room temperature water bath, and the corresponding SEM images of the final PLLA microspheres are shown in (d), (e), and (f).

After the volatilization of DCM, only irregular porous fragments were obtained, rather than PLLA spheres. This is attributed to the rapid freezing, which makes the emulsion droplets lose stability and break up during the solidification process (Shi and Weitz 2017; Werner *et al*. 2021). The surface instability and the morphology damage also occurred when the surrounding temperature rose to room temperature. As presented in Fig. 1 (f), no PLLA spheres were observed in the SEM images, instead irregular lumps

appeared. This is because of the high surrounding temperature, the volatilization rate of the DCM is quite high, and the volatilization can be completed in several minutes, leading to the instability of droplet morphology (Hung *et al*. 2010; Kuehne and Weitz 2011). When the surrounding temperature was around zero degrees, corresponding to ice water bath, the surface instability could be suppressed. After the steady volatilization of DCM and phase separation, the PLLA emulsion droplets were solidified and transformed into spheres. As shown in Fig. 1 (b) and 1(e), the droplets collected from the beaker had good sphericity and high dispersity. After the DCM volatilization, the droplets underwent stirring in a hot water bath, followed by repeated washing and freeze-drying. Finally, the PLLA spheres with regular shape were obtained, and the diameter of the spheres was around 250 μm. The successful fabrication of regular spheres is attributed to the flow stability inside the droplets and the slow volatilization of DCM. Therefore, 0 °C (ice water bath) would be a proper surrounding temperature for the droplet collection and solidification in the fabrication process of PLLA spheres.

Emulsification Method Optimization

Based on the above success, pore-forming agent (gelatin) was introduced so as to prepare microporous PLLA spheres. To obtain the desired pore structures and thus to meet application requirements, the influence of the dosage of the pore-forming agents was explored. The gelatins with the dosages of 2.5 wt%, 5 wt%, 7.5 wt%, and 10 wt% were respectively dissolved in the PVOH solution, and then introduced to the emulsion through 30 min ultrasonic emulsification. The obtained PLLA spheres and the corresponding surface structures are presented as SEM images in Fig. 2. As can be observed in Figs. 2 (a), 2 (c), 2 (e), and 2 (g), despite different dosages of pore-forming agents, all the obtained spheres maintained a regular shape with the size of approximately 250 μm, similar to those obtained without the addition of pore forming agents. This is because in such a microfluidic T-junction, the size of the generated droplet is mainly controlled by the T-junction geometry, the viscosity ratio, and flow rates of the dispersed phase and continuous phase. In the fabrication process, gelatin as the pore-forming agent almost had no effect on the droplet generation and the macroscopic morphology of the subsequently formed spheres. However, for the micro-structure, different dosages of gelatin led to different outcomes. Specifically, as shown in Figs. 2 (b), 2 (d), 2 (f), and 2 (h), when a small dosage of gelatin (2.5 wt% or 5 wt%) was introduced into the emulsion, no microporous structures were identified on the sphere surface. The failure of pore-forming agents in microstructure regulation may be attributed to excessive vibration and energy input caused by ultrasonic emulsification (Czekalska *et al.* 2021; Ge *et al*. 2016; Huang *et al*. 2017; Zhang *et al*. 2020). After the volatilization of DCM, the gelatin particles did not penetrate into the sphere, resulting in the formation of a complete PLLA shell after the emulsion droplet was solidified. The shell prevented the gelatin inside the sphere from dissolving in hot water bath, making it impossible to complete the construction of porous structure. When the dosage increased to 7.5 wt%, despite excessive vibration and energy input, some gelatin particles could penetrate the sphere and were dispersed on the sphere surface, which enable the gelatin to obtain the channels dissolving in hot water and thus create porous structure. The porous structure observed in Fig. 2 (f) means a successful regulation of microstructure, with the pore size of approximately 1.0 μm. With further increasing gelatin dosage to 10 wt%, the pore size was only increased to around 3 μm, indicating ineffective regulation of pore structure, and at the same time the shape of spheres was no longer maintained, which can be seen from the SEM images displayed in Figs. 2 (g) and 2 (h). The little change in

pore structure, albeit a significant increase in the dosage of pore-forming agents, may be because the function of the pore-forming agents is hindered by the overpowering effect of the ultrasonics in the emulsification method.

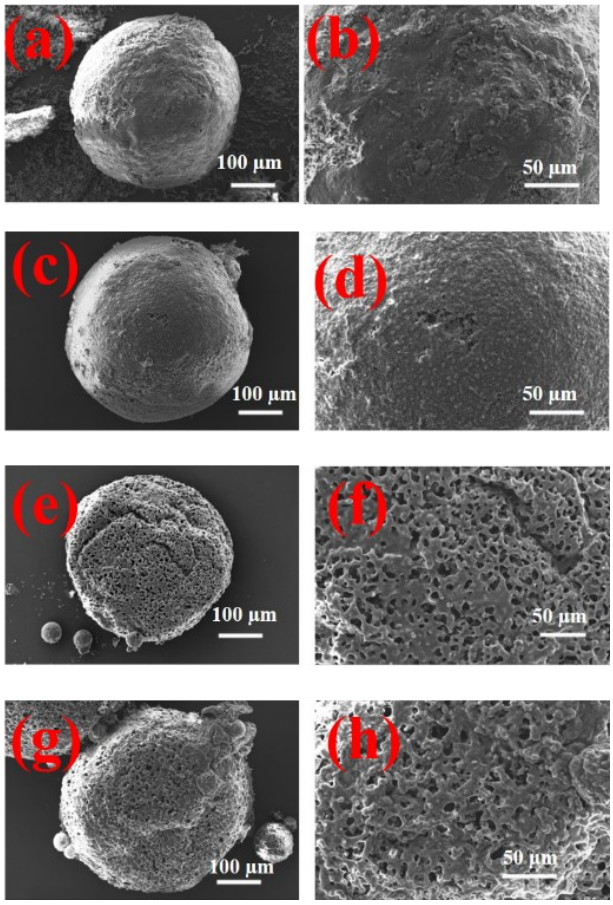

Fig. 2. SEM images of PLLA spheres obtained by different amount of pore-introducing agent: (a) 2.5 wt% gelatin, (c) 5 wt% gelatin, (e) 7.5 wt% gelatin and (g) 10 wt% gelatin, and the corresponding magnified images showing the sphere surfaces are (b), (d), (f), and (h), respectively

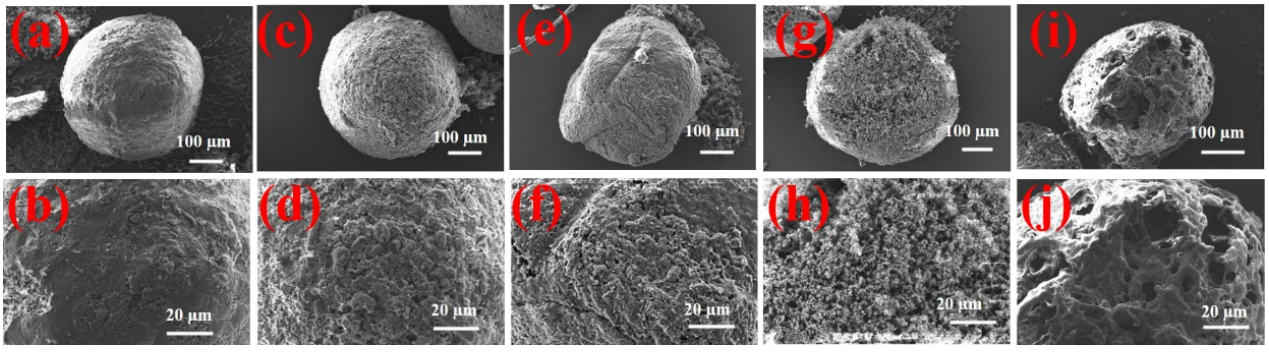

Fig. 3. SEM images of PLLA spheres obtained by different methods of emulsification: (a) 30 min ultrasonic emulsification, (c) 10 min ultrasonic emulsification, (e) 5 min ultrasonic emulsification, (g) 1 min ultrasonic emulsification and (i) 30 min high speed mechanical stirring (2500 rpm) for emulsification. The corresponding magnified images showing the sphere surfaces are (b), (d), (f), (h) and (j), respectively.

To verify the assumption that the ultrasonic emulsification for 30 min may provide an overpowering effect and thereby impede the pore structure forming, the ultrasonic emulsification with shorter time and the emulsification method with lower power consumption were explored. The dosage of the pore forming agent gelatin was fixed at 7.5 wt%, and the post-treatment with surrounding temperature of zero degree (ice water bath) to solidification, the volatilization, and the final hot water bath remained unchanged. Four different ultrasonic emulsification times, namely T=30, 10, 5, and 1.0 min, were considered, and a high-speed mechanical stirring of 30 min, as a representative of the emulsification method with lower power consumption, was also used for emulsification. Figure 3 shows the morphologies and surface structures of the generated spheres. When the ultrasonic emulsification time was reduced from 30 min to 10 or 5 min, the morphology of the obtained spheres roughly remained unchanged, typically with the size of around 250 μm and without porous structure, as can be seen from the SEM images in Figs. 3 (a)-(f). Upon further reducing the ultrasonic emulsification time to 1.0 min, the size of spheres remained, but small pores with diameter of about 1.0 μm appeared on the sphere surface (see Figs. 3 (g) and 3 (h)). These results can be explained as follows: regardless of the emulsification time, the ultrasonic emulsification always has excessive energy, which destroys the ability of the pore-forming agent to create microstructure.

Then, 30 min high-speed mechanical stirring emulsification was adopted instead of the ultrasonic emulsification, and the obtained PLLA spheres are shown in Figs. 3 (i) and 3 (j). Evidently, the size of the spheres remained roughly at 250 μm, while the porous structure changed dramatically, with a large number of 10 μm pores observed on the sphere surface. The change in porous structure indicates that the pore-forming function of gelatin was not hindered by this emulsification method, which may be attributed to the following reasons. The vibrations generated and the input energy induced by the mechanical stirring were small, although its speed was up to 2500 r/min. Thus, the gelatin in the emulsion could maintain the shape of small particles, and these particles penetrated the sphere after solidification (Gallassi *et al.* 2019). Under this condition, the pore-forming agents could fully utilize their pore-forming ability. Therefore, the high-speed mechanical stirring is a better choice to regulate the microstructure.

Pore Size Regulation *via* Gelatin Dosage

After clarifying the impact of emulsification methods on the pore-forming function of pore-forming agents, the dosage of pore forming agent gelatin was adjusted. The goal was to explore how it influences the pore structure. In the experiment, 2.5 wt%, 5 wt%, and 7.5 wt% gelatin dosages were respectively added into the original solution and emulsified with the 5 min high-speed mechanical stirring at 2500 rpm. Figure 4 shows SEM images of the PLLA spheres obtained at different dosages of gelatin. When the dosage of gelatin was 2.5wt%, regular spheres with the size of 250 μm were obtained, and numerous small pores of 3 to 5 μm were distributed on the sphere surface (Fig. 4 d). As the dosage of gelatin was increased to 5 wt%, the regular spheres with the size of around 250 μm were maintained, but small pores with the size of several micrometers were no longer observed on the sphere surface (Fig. 4 e). Instead, larger pore structures with diameter of 20 to 50 μm were clearly seen. When the dosage of gelatin was further increased to 7.5 wt%, the regular spheres with size of about 250 μm were still obtained. However, there were no small pores of several microns (Fig. 4 f), and the pores showing abnormally large size (100 μm) spread over the sphere surface, leading to a large number

of hollow structures inside the sphere. The increase in the size of pore structure was probably attributable to the increase in the size of gelatin particles caused by the high concentration in the emulsion. From the above results, it is apparent that the change in pore size was very sensitive to the dosage of gelatin. This also confirmed the above observation that the ultrasonic emulsification method destroys the formation and distribution of gelatin particles on the sphere surface, thereby losing the ability to regulate the pore structure (Wang *et al.* 2014; Ma 2019).

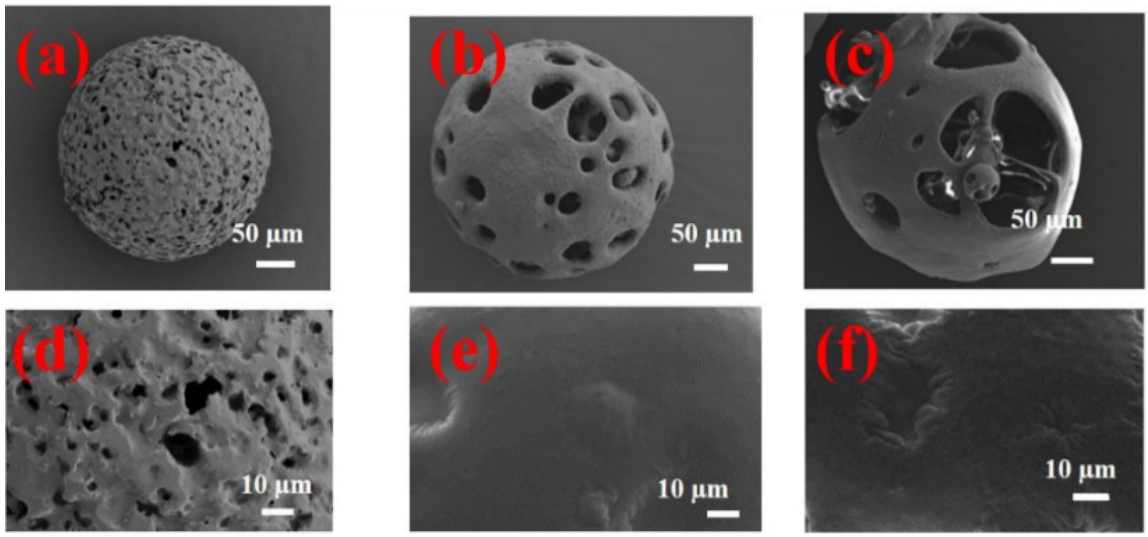

Fig. 4. SEM images of PLLA spheres obtained by different dosages of pore-forming agent: (a) 2.5 wt% gelatin, (b) 5 wt% gelatin, (c) 7.5 wt% gelatin. The corresponding magnified images showing the sphere surface are (d), (e) and (f). High speed mechanical stirring was used for emulsification.

It is indicated in Fig. 4 that when emulsified by the 5 min high-speed mechanical stirring, the dosage of the pore-forming agent gelatin almost had no effect on the final particle size but that it had a significant impact on the pore size on the sphere surface. To quantify the pore size change, the surface pore size distribution was extracted by the Image J software from the SEM images. The pore sizes were defined as equivalent circular diameters, which were calculated by the surface area, and more than 50 micro-pores were selected. Figure 5 exhibits the surface pore size distributions of PLLA spheres obtained with different dosages of the pore-forming agent gelatin.

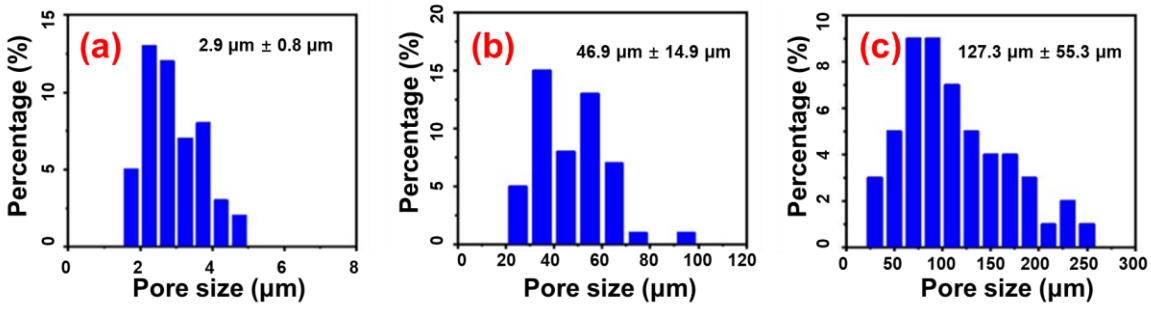

Fig. 5. Surface pore size distributions of PLLA spheres obtained by different dosages of pore-forming agent: (a) 2.5 wt% gelatin, (b) 5 wt% gelatin, and (c) 7.5 wt% gelatin. High-speed mechanical stirring was used for emulsification.

It can be seen that a low dosage of gelatin (2.5 wt%) resulted in small pores sized at 2 to 5 μm and averaged at 2.9±0.8 μm. By contrast, 5 wt% gelatin resulted in larger pores sized at 20 to 80 μm and averaged at 46.9±14.9 μm, and 7.5 wt% gelatin resulted in the largest pores sized at 40 to 250 μm and averaged at 127.3±55.3 μm. Due to the limitation of the sphere size, the confidence interval widened when regulating for larger pores.

Optical photographs were taken to monitor the hollow structures inside the PLLA spheres in Fig. 6. The pore-forming agent gelatin not only can induce the pore structure on the surface of the sphere, but it also can permit light transmission, which may indicate the creation of hollow structure inside the sphere. Figure 6 showed the inner hollow structure of the small-pore, middle-pore, and large-pore structured spheres obtained by using different dosages of gelatin. Clearly, the small-pore structured spheres possessed the lowest light transmittance (Fig. 6 a), while the large-pore structured spheres possessed the highest light transmittance (Fig. 6 c), indicating that as the surface pore size increases, the hollow structure inside the sphere increases.

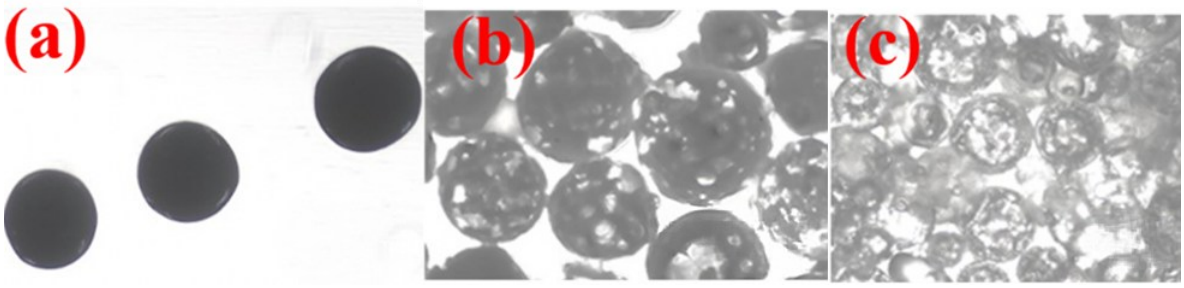

Fig. 6. Optical photographs of PLLA spheres obtained by different dosages of pore-forming agent: (a) 2.5 wt% gelatin, (b) 5 wt% gelatin, and (c) 7.5 wt% gelatin, corresponding to Fig.4 (a),(b) and (c).

In order to better demonstrate the morphology of microspheres with different pore structures, the specific surface area of microspheres with different pore structures was measured by the BET test. Table 1 lists the measurements of the specific surface area of the microspheres with three different pore structures by the adsorption test or the desorption test, respectively defined as S_a and S_d. It is shown that both S_a and S_d increased with the size of the pore structure, which is reasonable since the fact that the appearance of large pore structures reduces the variability and the specific surface area of the surface of the microspheres. This is consistent with the theory of the relationship between pore structure and specific surface area in previous studies (Zhang *et al*. 2015b; Boyjoo *et al*. 2016).

Table 1. Specific Surface Area of PLLA Microspheres with Different Pore Sizes *via* BET

Sample	S_a / $m^2 \cdot g^{-1}$	S_d / $m^2 \cdot g^{-1}$
PLLA-small pores (2.5 wt%)	0.42156	5.1058
PLLA-medium pores (5 wt%)	0.26323	3.5032
PLLA-large pores (7.5 wt%)	0.13602	2.5427

Universality Assessment

In addition to the ability to regulate the morphology of microspheres, the universality of microfluidic preparation methods has also received attention. Therefore, an attempt to prepare porous microspheres by sequentially replacing the PLLA matrix with two other types of polymers, *i.e.*, PNAGA and PCL were undertaken. Like in the preparation of porous PLLA microspheres, the 5 min high-speed mechanical stirring was used for emulsification, the dosage of pore-forming agent was set as 5 wt%, and the surfactants and solvent remained unchanged. The experimental results indicated that the other two polymer microspheres, like PLLA microspheres, also could be successfully prepared. Figure 7 reveals the morphologies and surface appearances of the PNAGA and PCL microspheres. Different from the PLLA microspheres, the PNAGA microspheres exhibited elliptical shapes with slightly larger size, and a fibrous structure rather than a pore structure was observed on the surface of PNAGA microspheres (see Figs. 7 a and 7 b). These differences were probably due to the higher viscosity and surface tension of the PNAGA solution, which leads to the formation of larger droplets and ultimately to the solidification into larger spheres (Liu and Ma 2010; Zhang *et al.* 2015b). During the solidification process of droplets, the high viscosity also induces stronger interactions inside the droplets, resulting in stronger entanglement on the surface of the microspheres and ultimately leading to a fibrous structure. The morphology of PCL microspheres was similar to that of PLLA microspheres, except that the surface pore size was slightly reduced (14.3 ± 3.9 μm, see Figs. 7 c and 7 d). Some wrinkles were apparent on the sphere surface, which may be caused by different curing shrinkage rates of different components inside the droplet during the solidification process (Wang *et al.* 2019). The successful preparation of PNAGA and PCL microspheres with pore structures indicates that the proposed microfluidic methods are universal for various preparations.

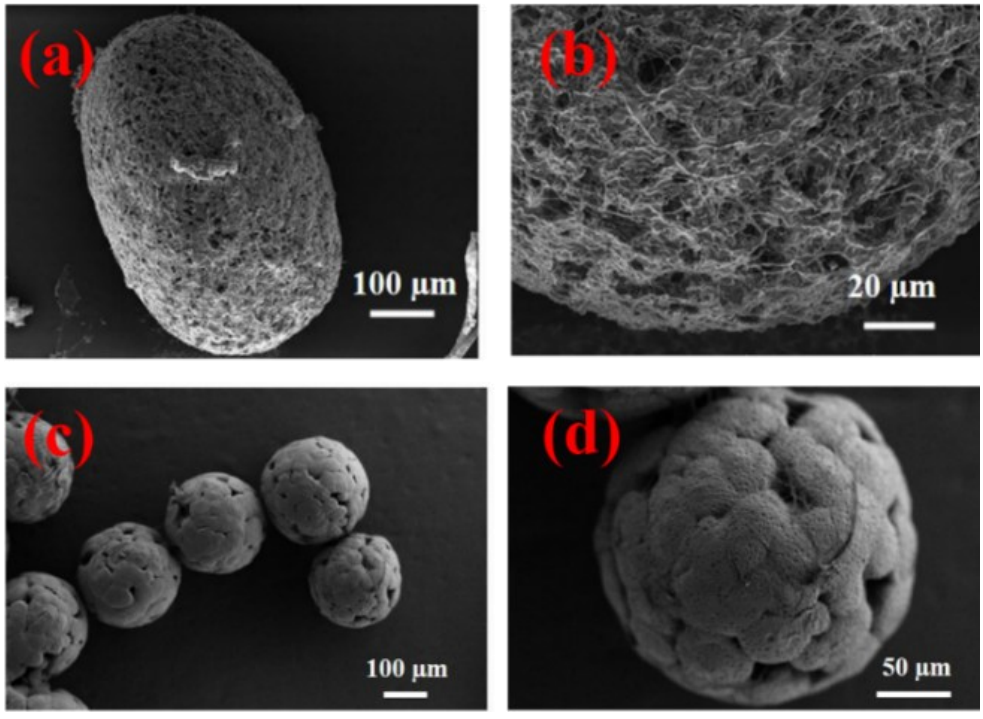

Fig. 7. SEM images of (a-b) PNAGA and (c-d) PCL microspheres obtained with the proposed microfluidic method

CONCLUSIONS

In this study, a microfluidic method for the fabrication of poly(L-lactic acid) (PLLA) spheres with specific micropore structure was explored and evaluated.

1. In this method, poly(vinyl alcohol) (PVOH) solution was used as the continuous phase, and an emulsion containing matrix materials (PLLA), stabilizer (sorbitan monooleate) and pore-forming agents (gelatin) dissolved in dichloromethane (DCM) were emulsified to be dispersed phase for the generation of droplets, such that they were eventually transformed into microspheres. The droplets needed to be collected in an ice water bath environment to maintain their stability, after which they were solidified into complete PLLA microspheres.
2. Regardless of the dosage of the pore-forming agent, the ultrasonic emulsification always hindered the formation of surface pore structures and internal hollow structures. This effect was attributed to excessive vibration and high energy input, which would make the pore-forming agent in the emulsion fully penetrate the microspheres, thus losing the ability to adjust the porous structure in the subsequent droplet solidification process.
3. Mechanical stirring was shown to be a more suitable emulsification method. That approach was combined with different amounts of pore-forming agents (2.5wt%, 5wt%, and 7.5wt% gelatin) to prepare microspheres with various structures. Three types of spheres with different micropore structures (small: 2.9±0.8 μm, middle: 46.9±14.9 μm, and large: 127.3±55.3 μm) were successfully obtained.
4. The proposed microfluidic method was also applied to prepare porous structural spheres of poly(N-acryloyl glycinamide) (PNAGA) and poly(caprolactone) (PCL), indicating its universality and application prospects in industrial regulation and preparation of various polymer microspheres. This research would lay a solid foundation for facilitating the microfluidic fabrication into commercial applications.

ACKNOWLEDGEMENTS

The authors gratefully acknowledge the support of the Free Exploration Basic Research Project of Shaanxi (No. 2024ZY-JCYJ-01-02), the National Key R&D Program of China (No. 2022YFF0503500), the Major Special Science and Technology Project of the Inner Mongolia Autonomous Region (No. 2020ZD0022).

Declaration of Competing Interest

The authors declare that they have no known competing financial interests or personal relationships that could have appeared to influence the work reported in this paper.

Conflicts of Interest

There are no conflicts to declare.

REFERENCES CITED

Aghaei, H., Solaimany Nazar, A. R., and Varshosaz, J. (2021). "Double flow focusing microfluidic-assisted based preparation of methotrexate–loaded liposomal nanoparticles: Encapsulation efficacy, drug release and stability," *Colloids and Surfaces A: Physicochemical and Engineering Aspects* 614, article 126166. DOI: 10.1016/j.colsurfa.2021.126166.

Bao, Y., Zhang, Y., and Ma, J. (2020). "Reactive amphiphilic hollow SiO_2 Janus nanoparticles for durable superhydrophobic coating," *Nanoscale* 12(31), 16443-16450. DOI: 10.1039/d0nr02571b.

Barroca, N., Daniel-da-Silva, A. L., Vilarinho, P. M., and Fernandes, M. H. V. (2010). "Tailoring the morphology of high molecular weight PLLA scaffolds through bioglass addition," *Acta Biomater* 6(9), 3611-3620. DOI: 10.1016/j.actbio.2010.03.032.

Boyjoo, Y., Wang, M., Pareek, V. K., Liu J., and Jaroniec M. (2016). "Synthesis and applications of porous non-silica metal oxide submicrospheres," *Chem. Soc. Rev*. 45(21), 6013-6047. DOI: 10.1039/C6CS00060F

Czekalska, M. A., Jacobs, A. M. J., Toprakcioglu, Z., Kong, L., Baumann, K. N., Gang, H., Zubaite, G., Ye, R., Mu, B., Levin, A., Huck, W. T. S., and Knowles, T. P. J. (2021). "One-step generation of multisomes from lipid-stabilized doubleemulsions," *ACS Appl. Mater. Interfaces* 13(5), 6739-6747. DOI: 10.1021/acsami.0c16019

Dai, X., Zhao, X., Liu, Y., Chen, B., Ding, X., Zhao, N., and Xu, F.J. (2021). "Controlled synthesis and surface engineering of janus chitosan-gold nanoparticles for photoacoustic imaging-guided synergistic gene/photothermal therapy," *Small* 17(11), article 2006004. DOI: 10.1002/smll.202006004

Deng, X., Li, K., Cai, X., Liu, B., Wei, Y., Deng, K., Xie, Z, Wu, Z., Ma, P., Hou, Z., Cheng, Z., and Lin, J. (2017). "A hollow-structured CuS@Cu_2S@Au nanohybrid: Synergistically enhanced photothermal efficiency and photoswitchable targeting effect for cancer theranostics," *Adv. Mater*. 29(36), article 1701266. DOI: 10.1002/adma.201701266

de Carvalho, B. G., Taketa, T. B., Garcia, B. B. M., Han, S. W., and de la Torre, L. G. (2021). "Hybrid microgels produced *via* droplet microfluidics for sustainable delivery of hydrophobic and hydrophilic model nanocarriers," *Mater. Sci. Eng. C Mater. Biol. Appl*. 118, article 111467. DOI: 10.1016/j.msec.2020.111467

Elsayed, M., Kothandaraman, A., Edirisinghe, M., and Huang, J. (2016). "Porous polymeric films from microbubbles generated using a T-junction microfluidic device," *Langmuir* 32(50), 13377-13385. DOI: 10.1021/acs.langmuir.6b02890

Fales, A. M., Yuan, H., and Vo-Dinh, T. (2011). "Silica-coated gold nanostars for combined surface-enhanced Raman scattering (SERS) detection and singlet-oxygen generation: A potential nanoplatform for theranostics," *Langmuir* 27(19), 12186-12190. DOI: 10.1021/la202602q

Gallassi, M., Gonçalves, G. F. N., Botti, T. C., Moura, M. J. B., Carneiro, J. N. E., and Carvalho, M. S. (2019). "Numerical and experimental evaluation of droplet breakage of O/W emulsions in rotor-stator mixers," *Chemical Engineering Science* 204, 270-286. DOI: 10.1016/j.ces.2019.04.011

Ge, L., Friberg, S. E., and Guo, R. (2016). "Recent studies of Janus emulsions prepared by one-step vibrational mixing," *Current Opinion in Colloid & Interface Science* 25, 58-66. DOI: 10.1016/j.cocis.2016.05.001

Geng, Y., Ling, S. D., Huang, J., and Xu, J. (2020). "Multiphase microfluidics:

fundamentals, fabrication, and functions," *Small*, 16(6), article 1906357. DOI: 10.1002/smll.201906357

Huang, X., Eggersdorfer, M., Wu, J., Zhao, C.-X., Xu, Z., Chen, D., and Weitz, D. A. (2017). "Collective generation of milliemulsions by step-emulsification," *RSC Advances* 7(24), 14932-14938. DOI: 10.1039/c7ra00935f

Hung, L. H., Teh, S. Y., Jester, J., and Lee, A. P. (2010). "PLGA micro/nanosphere synthesis by droplet microfluidic solvent evaporation and extraction approaches," *Lab on a Chip* 10(14), 1820-1825. DOI: 10.1039/c002866e

Ježková, M., Jelínek, P., Marelja, O., Trunov, D., Jarošová, M., Slouka, Z., and Šoóš, M. (2022). "The preparation of mono- and multicomponent nanoparticle aggregates with layer-by-layer structure using emulsion templating method in microfluidics," *Chemical Engineering Science* 247, article 117084. DOI: 10.1016/j.ces.2021.117084

Jing, J., Zhang, X., Gao, L., Gao, F., Huo, H., Shi, S., Cheng, W., Xu, C., Wang, J., and An, C. (2023). "Continuous preparation of multi-scale HMX-based energetic composite microspheres by pipe-stream technology," *Powder Technology* 426, article 118640. DOI: 10.1016/j.powtec.2023.118640

Joseph, X., Akhil, V., Arathi, A., and Mohanan, P. V. (2022). "Microfluidic synthesis of gelatin nanoparticles conjugated with nitrogen-doped carbon dots and associated cellular response on A549 cells," *Chem. Biol. Interact*. 351, article 109710. DOI: 10.1016/j.cbi.2021.109710

Kim, D. Y., Jin, S. H., Jeong, S. G., Lee, B., Kang, K. K., and Lee, C. S. (2018). "Microfluidic preparation of monodisperse polymeric microspheres coated with silica nanoparticles," *Sci. Rep*. 8(1), article 8525. DOI: 10.1038/s41598-018-26829-z

Kuehne, A. J. C., and Weitz, D. A. (2011). "Highly monodisperse conjugated polymer particles synthesized with drop-based microfluidics," *Chemical Communications (Camb)* 47(45), 12379-12381. DOI: 10.1039/c1cc14251h

Li, G., Cheng, R., Cheng, H., Yu, X.-Q., Ling, L., Wang, C.-F., and Chen, S. (2021). "Microfluidic synthesis of robust carbon dots-functionalized photonic crystals," *Chemical Engineering Journal* 405, article 126539. DOI: 10.1016/j.cej.2020.126539.

Liu, X., and Ma, P. X. (2010). "The nanofibrous architecture of poly(L-lactic acid)-based functional copolymers," *Biomaterials* 31(2), 259-69. DOI: 10.1016/j.biomaterials.2009.09.046

Liu, H., Qian, X., Wu, Z., Yang, R., Sun, S., and Ma, H. (2016). "Microfluidic synthesis of QD-encoded PEGDA microspheres for suspension assay," *J. Mater. Chem. B* 4(3), 482-488. DOI: 10.1039/c5tb02209f

Liu, Y., Yang, G., Hui, Y., Ranaweera, S., and Zhao, C.X. (2022). "Microfluidic nanoparticles for drug delivery," *Small* 18(36), article 2106580. DOI: 10.1002/smll.202106580

Ma, S. (2019). "Gelatin-based microfluidics device with the feature sizes smaller than 100 μm for production of oil-in-water emulsions," *Microfluidics and Nanofluidics*, 23(3), article 35. DOI: 10.1007/s10404-019-2203-4

Maeki, M., Uno, S., Niwa, A., Okada, Y., and Tokeshi, M. (2022). "Microfluidic technologies and devices for lipid nanoparticle-based RNA delivery," *J. Control Release* 344, 80-96. DOI: 10.1016/j.jconrel.2022.02.017

Nie, T. T., He, M., Ge, M., Xu, J. Z., and Ma, H. Y. (2017). "Fabrication and structural regulation of PLLA porous microspheres *via* phase inversion emulsion and thermally induced phase separation techniques," *Inc. J. Appl. Polym. Sci.* 134, article 44885. DOI: 10.1002/app.44885

Prasad, N., Perumal, J., Choi, C.-H., Lee, C.-S., and Kim, D.-P. (2009). "Generation of monodisperse inorganic-organic Janus microspheres in a microfluidic device," *Advanced Functional Materials* 19(10), 1656-1662. DOI: 10.1002/adfm.200801181

Purbia, R., and Paria, S. (2015). "Yolk/shell nanoparticles: classifications, synthesis, properties, and applications," *Nanoscale* 7(47), 19789-19873. DOI: 10.1039/c5nr04729c

Shi, W., and Weitz, D.A. (2017). "Polymer phase separation in a microcapsule shell," *Macromolecules* 50(19), 7681-7686. DOI: 10.1021/acs.macromol.7b01272

Shoji, R., Yoshida, S., Kikuchi, S., Kanehashi, S., Okamoto, K., Ma, G., and Ogino, K. (2021). "Microfluidic fabrication of polymer blend particles containing poly(4-butyltriphenylamine)-block-poly(methyl methacrylate): Effect of block copolymer and rate of solvent evaporation on morphology," *Colloid and Polymer Science* 299, 969-978. DOI: 10.1007/s00396-021-04817-6

Solsona, M., Vollenbroek, J. C., Tregouet, C. B. M., Nieuwelink, A. E., Olthuis, W., van den Berg, A., Weckhuysen, B. M., and Odijk, M. (2019). "Microfluidics and catalyst particles," *Lab Chip* 19(21), 3575-3601. DOI: 10.1039/c9lc00318e

Sommer, M. R., Schaffner, M., Carnelli, D., and Studart, A. R. (2016). "3D printing of hierarchical silk fibroin structures," *ACS Applied Materials & Interfaces* 8(50), 34677-34685. DOI: 10.1021/acsami.6b11440

Tahira, N., Madni, A., Li, W., Correia, A., Khan, M. M., Rahim, M. A., and Santos, H. A. (2020). "Microfluidic fabrication and characterization of Sorafenib-loaded lipid-polymer hybrid nanoparticles for controlled drug delivery," *International Journal of Pharmaceutics* 581, article 119275. DOI: 10.1016/j.ijpharm.2020.119275

Visaveliya, N., and Kohler, J. M. (2014). "Single-step microfluidic synthesis of various nonspherical polymer nanoparticles *via in situ* assembling: dominating role of polyelectrolytes molecules," *ACS Appl. Mater. Interfaces* 6(14), 11254-11264. DOI: 10.1021/am501555y

Wang, C.-C., Yang, K.-C., Lin, K.-H., Wu, C.-C., Liu, Y.-L., Lin, F.-H., and Chen, I.-H. (2014). "A biomimetic honeycomb-like scaffold prepared by flow-focusing technology for cartilage regeneration," *Biotechnology and Bioengineering* 111(11), 2338-2348. DOI: 10.1002/bit.25295

Wang, J., Cheng, Y., Yu, Y., Fu, F., Chen, Z., Zhao, Y., and Gu, Z. (2015). "Microfluidic generation of porous microcarriers for three-dimensional cell culture," *ACS Applied Materials & Interfaces* 7(49), 27035-27039. DOI: 10.1021/acsami.5b10442

Wang, J., Le-The, H., Wang, Z., Li, H., Jin, M., van den Berg, A., Zhou, G., Segerink, L .I., Shui, L., and Eijkel, J. C. T. (2019). "Microfluidics assisted fabrication of three-tier hierarchical microparticles for constructing bioinspired surfaces," *ACS Nano* 13(3), 3638-3648. DOI: 10.1021/acsnano.9b00245

Werner, J. G., Lee, H., Wiesner, U., and Weitz, D. A. (2021). "Ordered mesoporous microcapsules from double emulsion confined block copolymer self-assembly," *ACS Nano* 15(2), 3490-3499. DOI: 10.1021/acsnano.1c00068

Wu, Y., Li, Y., Qin, L., Yang, F. L., Wu, D. C. (2013). "Monodispersed or narrow-dispersed melamine-formaldehyde resin polymer colloidal spheres: Preparation, size-control, modification, bioconjugation and particle formation mechanism," *J. Mater. Chem. B* 1(2), 204-212. DOI: 10.1039/C2TB00043A

Xu, Q., Hashimoto, M., Dang, T. T., Hoare, T., Kohane, D. S., Whitesides, G. M., Langer, R., and Anderson, D. G. (2009). "Preparation of monodisperse biodegradable polymer microparticles using a microfluidic flow-focusing device for controlled drug

delivery," *Small* 5(13), 1575-1581. DOI: 10.1002/smll.200801855.

Zeng, Y., Li, X., Liu, X., Yang, Y., Zhou, Z., Fan, J., and Jiang, H. (2021). "PLLA porous microsphere-reinforced silk-based scaffolds for auricular cartilage regeneration," *ACS Omega* 6(4), 3372-3383. DOI: 10.1021/acsomega.0c05890.

Zhang, F., Liao, P., Sun, Y., Chen, Z., Pang, Y., and Huang, Y. (2020). "Surfactant and oil formulations for monodisperse droplet emulsion PCR," *Lab Chip* 20(13), 2328-2333. DOI: 10.1039/d0lc00052c.

Zhang, Z., Gupte, M. J., Jin, X., and Ma, P. X. (2015a). "Injectable peptide decorated functional nanofibrous hollow microspheres to direct stem cell differentiation and tissue regeneration," *Adv. Funct. Mater*. 25(3), 350-360. DOI: 10.1002/adfm.201402618.

Zhang, M., Wang, W., Yang, X., Ma, B., Liu, Y. M., Xie, R., Ju, X. J., Liu, Z., and Chu, L.Y. (2015b), "Uniform microparticles with controllable highly interconnected hierarchical porous structures," *ACS Appl. Mater. Inter*. 7(25), 13758-13767. DOI: 10.1021/acsami.5b01031.

Zhao, Q., Cui, H., Wang, Y., and Du, X. (2020). "Microfluidic platforms toward rational material fabrication for biomedical applications," *Small* 16(9), article 1903798. DOI: 10.1002/smll.201903798.

Zhao, Z., Li, G., Ruan, H., Chen, K., Cai, Z., Lu, G., Li, R., Deng, L., Cai, M., and Cui, W. (2021a). "Capturing magnesium ions *via* microfluidic hydrogel microspheres for promoting cancellous bone regeneration," *ACS Nano* 15(8), 13041-13054. DOI: 10.1021/acsnano.1c02147.

Zhao, Z., Wang, Z., Li, G., Cai, Z., Wu, J., Wang, L., Deng, L., Cai, M., and Cui, W. (2021b). "Injectable microfluidic hydrogel microspheres for cell and drug delivery," *Advanced Functional Materials* 31(31), article 2103339. DOI: 10.1002/adfm.202103339.

Zhou, J., Zhai, Y., Xu, J., Zhou, T., and Cen, L. (2021). "Microfluidic preparation of PLGA composite microspheres with mesoporous silica nanoparticles for finely manipulated drug release," *Int. J. Pharm*. 593, article 120173. DOI: 10.1016/j.ijpharm.2020.120173.

Ziemecka, I., van Steijn, V., Koper, G.J., Rosso, M., Brizard, A. M., van Esch, J. H., and Kreutzer, M. T. (2011). "Monodisperse hydrogel microspheres by forced droplet formation in aqueous two-phase systems," *Lab Chip* 11(4), 620-624. DOI: 10.1039/c0lc00375a.

Zou, L., Huang, B., Zheng, X., Pan, H., Zhang, Q., Xie, W., Zhao, Z., and Li, X. (2022). "Microfluidic synthesis of magnetic nanoparticles in droplet-based microreactors," *Materials Chemistry and Physics* 276, article 125384. DOI: 10.1016/j.matchemphys.2021.125384.

Article submitted: April 6, 2025; Peer review completed: May 18, 2025; Revised version received: July 10, 2025; Accepted: July 12, 2025; Published: August 27, 2025.
DOI: 10.15376/biores.20.4.9063-9078